International Research Journal of Innovations in Engineering and Technology (IRJIET)

ISSN (online): 2581-3048
Volume 7, Issue 7, pp 165-177, July-2023
https://doi.org/10.47001/IRJIET/2023.707026

Energy, Exergy, and Exergoeconomic Analysis of a Combined Recompression Supercritical Carbon Dioxide Brayton-Organic Rankine Cycle for Waste Heat Recovery

Oku Ekpenyong Nyong

Department of Mechanical Engineering, University of Cross River State, Calabar, Nigeria
Author's E-mail: nyong.oku@gmail.com

HIGHLIGHTS

- An energy, exergy, and exergoeconomic analysis is performing for combined recompression sCO_2-ORC cycle.
- R245fa is obtained as the most suitable working fluid for the sCO_2-ORC cycle in terms of performance, exergoeconomic analysis of the system.

Abstract **- In this study, an energy, exergy and exergoeconomic analyses of combined recompression supercritical carbon dioxide and organic Rankine cycle (SCO_2/ORC) for waste heat recovery application is presented. The impact of $P_1, T_1, \dot{m}_{co2}, \varepsilon_{LTR}$ and ε_{HTR} on the system's thermodynamic and exergoeconomic performance is investigated. The working fluid used for the bottoming cycle of the SCO_2/ORC system is R245fa. Results obtained shows that a maximum $W_{Net}, \eta_{th}, \eta_{ex}$ of 1088kW, 47.11%, 58.81% and minimumc_{elect} of 4.274$/GJ at different operating conditions is achievable. Also we observe that increasing the inlet pressure by 10kPa leads to the increase of about 251.3kW of net power, 1.89%pt. increase of η_{th} and 5.165h/GJ of $\dot{Z}_{overall} + \dot{C}_{D,overall}$, and decreases η_{ex} and c_{elect} by 1.89%pt. and 1.618$/GJ, respectively. Similarly, increasing T_1 shows an increasing influence on $W_{Net}, \eta_{th}, \eta_{ex}$ and $f_{overall}$ while the reverse trend is experience for $c_{elect}, \dot{C}_{D,overall}$ and $\dot{Z}_{overall} + \dot{C}_{D,overall}$.**

Keywords: Exergy efficiency, exergoconomic performance, thermal efficiency, and recompression supercritical carbon dioxide.

1. Introduction

The drive for carbon dioxide (CO_2) reduction and more efficient energy utilization have spurred increases attention in the effective utilization of low and medium grade temperature heat for electricity generation, heating or cooling purposes. The supercritical carbon dioxide (SCO_2) is a promising option for high efficiency power generation with potential applications for exhaust waste heat recovery [1][2][3], nuclear [4][5], coal-fired [6][7], and renewable energy such as geothermal [8][9] , solar thermal[10][11], and fuel cells[12]. The SCO_2 cycle has unique advantage because of its characteristics compactness, simplicity, sustainability, superior economic, and enhanced safety[13][3]. The thermo-physical properties of CO_2 has no temperature limitation of decomposition and produces minimum compressor work near the critical point, hence capable of achieving significantly high efficiency even at the same turbine inlet temperature[3][2]. For SCO_2 cycles with high temperature heat source (300-600^{0}C), the recuperator is used to increase the maximum cycle temperature to levels such that high cycle efficiency is achieved. This temperature rise is through the heat transfer from the turbine exhaust stream (with low specific heat) to the pump exit stream (with high specific heat), therefore creating internal irreversibility in the recuperator due to large variation in specific heat capacity between the two streams[1]. To accommodate for this changes in heat capacity, the recompression SCO_2 cycle uses the high temperature recuperator (HTR) and low temperature recuperator (LTR) with different flow rates to compensate for the low heat capacity in the turbine exhaust stream and minimize exergy destruction in the recuperator. The additional energy in the LTR exit stream can be utilized by a low temperature system such as organic Rankine cycle (ORC) in a combined SCO_2/ORC configuration to compensate for the low heat capacity.

Some researchers have conducted studies on combined SCO_2 Brayton cycle and ORC configurations to utilize waste exhaust heat from the SCO_2 cycle therefore, maximizing overall performance. Besarati and Goswami[14]investigated the performance of different SCO_2 configurations and concluded that the recompression and partial cooling SCO_2 configuration have better performance compared to the single SCO_2 configuration, with high efficiency of about 50%. And further revealed that even higher efficiency of 55% can be

International Research Journal of Innovations in Engineering and Technology (IRJIET)

ISSN (online): 2581-3048

Volume 7, Issue 7, pp 165-177, July-2023

https://doi.org/10.47001/IRJIET/2023.707026

achieved in combined SCO_2/ORC configuration. Akbari and Mahmoudi[15]reported on the exergoeconomic analysis of a combined supercritical CO_2 recompression Brayton/organic Rankine cycle (SCRB/ORC). Their results revealed that the combined SCRB/ORC has 12% higher exergy efficiency than that of SCRB, and the best working fluid option were Isobutane and RC318. Wang and Dai [16]examined the exergoeconomic performance of two combined configuration, which are transcritical CO_2 (tCO_2) and ORC for waste heat recovery from the recompression SCO_2 cycle. Results reveal that at lower compression pressure ratio, the SCO_2/tCO_2 perform better than the SCO_2/ORC.Cao and Habibi[17] investigated the environmental and exergoeconomic performance of a proposed combined regenerative gas turbine cycle (GTC) and recompression supercritical CO_2 Brayton cycle (SCBC) powered by hybrid solar-biomass heat source and using a combination of thermoelectric generator, LiBr-H_2O and proton exchange membrane electrolyzer subsystems for waste heat recovery. The analysis was performed in two mode; hybrid and biomass-only mode. The reported results reveal that the overall system energy efficiency increased by 22.48 and 29.6%Pt., and the exergy efficiency increased by 6.18 and 7.6%Pt. for hybrid and biomass-only, respectively.

In the present study, energy, exergy and exergoeconomic-based parametric evaluation of combined recompression SCO_2/ORC system is perform, to investigate thermal and exergy efficiency, net power output and exergy cost rates at each flow stream and component. The innovative contribution of this work is in comparative analysis of the SCO_2 and combined SCO_2/ORC systems, and the exergoeconomic evaluation of SCO_2/ORC, thus analyzing the system from both technical and economic approach.

2. System Descriptions and Assumption

Fig. 1 shows the schematic diagram of the combined recompression-based supercritical carbon dioxide (SCO_2) and organic Rankine cycle (ORC) for waste heat recovery. The topping SCO_2 cycle consist of a gas heater, high-temperature (HTR) and low-temperature (LTR) recuperators, a pre-cooler, SCO_2 turbine and the main and recompression compressors, while the bottoming ORC cycle is comprised of a heat exchanger, and ORC turbine, a condenser and a pump. In the topping cycle, the recompression configuration is adapted because of it's enhance thermal efficiency due to its ability to reduce heat losses in the recompressed SCO_2 and use flow splitting to compensate for changes in specific heat in the LTR [13] The SCO_2 stream leaving the LTR (state 4) is split upstream; one portion with the higher mass flow rate passes through the heat exchanger (state 6 – 7) and cool in the pre-cooler (state 7 – 8) before entering the main compressor. The high pressure SCO_2 stream (state 9) exiting the main compressor flows through the LTR heat exchanger, absorbs heat from the incoming stream (state 3) before leaving (state 10). The remaining fraction of the split stream is directly compressed in the recompression compressor (state 5 – 11).The high pressure stream exiting the recompression compressor (state 11) mixes with the main stream returning through the LTR (state 10) prior to entering the HTR (state 12), and then absorbs heat from the incoming stream (state 2) before flowing to the gas heater (state 13) where is heated to SCO_2 turbine inlet temperature (state 1). After expansion the SCO_2 turbine exhaust (state 2) returns to the main and recompression compressor after releasing heat in the HTR and LTR heat exchangers.

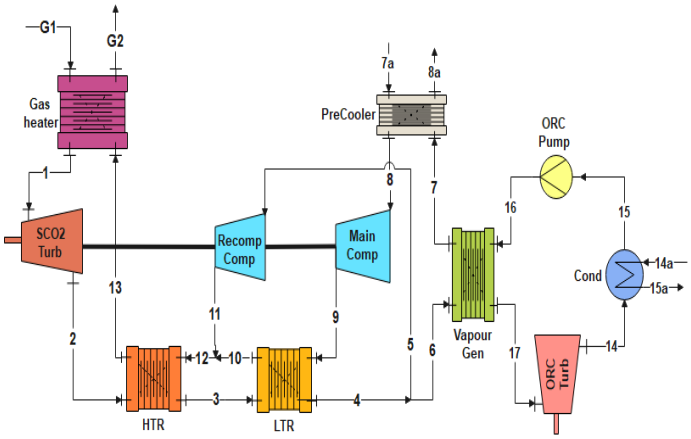

Fig.1: Schematic diagram of an SCO_2/ORC system for waste gas recovery

In the bottoming ORC cycle, the organic working fluid (state 15) is compressed in the pump to heat exchanger pressure (state 15), where it is heated to ORC turbine inlet temperature (state 17). The expanded working fluid exhaust (state 14) is then condensed in the condenser (state 15) and the entire process is repeated again. The SCO_2 in the SCO_2/ORC system absorbs heat from the gas turbine exhaust waste heat, while the ORC utilizes heat from the SCO_2turbine exhaust before entering the main compressor. This configuration is able to reduce waste heat release to the environment with improve energy conversion efficiency.

The following assumptions are adapted in this system simulation to simplify the calculations:

1) The system operates under steady-state condition.
2) Pressure drop in all heat exchangers are negligible except in the pump, compressor and turbines.
3) Heat transfer to the environment is negligible except in the pre-cooler unit.
4) The exhaust gas temperature should not be less than 120^0C to avoid acid dew point.
5) Changes in potential and kinetic energies are not negligible.

International Research Journal of Innovations in Engineering and Technology (IRJIET)

ISSN (online): 2581-3048

Volume 7, Issue 7, pp 165-177, July-2023

https://doi.org/10.47001/IRJIET/2023.707026

3. System Modeling

The SCO_2/ORC system is model based on energy and exergy balance in each component of the system. The performance simulation and calculation of physical properties of the fluids involve is perform with the help of Engineering Equation Solver (EES) developed by Ibrahim and Klein [18].

3.1 Thermodynamic model

The mass and energy conservation, as well as exergy balance relations for each system component are represented as [19]:

$$\sum \dot{m}_{in} = \sum \dot{m}_{out} \quad (1)$$

$$\sum \dot{m}_{in} h_{in} + \dot{Q}_{cv} - \sum \dot{m}_{out} h_{out} - \dot{W}_{cv} = 0 \quad (2)$$

$$\sum \dot{E}_{in} - \sum \dot{E}_{out} + \sum \dot{E}_{heat} + \sum \dot{W}_{J} - \dot{E}_{D,J} = 0 \quad (3)$$

The total exergy at each state point is the sum of the physical and chemical components, neglecting the potential and kinetic exergies it can be expressed as [19][20]:

$$\dot{E} = \dot{E}_{ph} + \dot{E}_{ch} \quad (4)$$

The specific physical and chemical exergy is defined as:

$$\dot{E}_{ph} = \dot{m}[(h - h_0) - T_0(s - s_0)] \quad (5)$$

$$\dot{E}_{ch} = \dot{m}\left[\sum_{i=1}^{n} X_i \, ex_{ch,i} + RT_0 \sum_{i=1}^{n} X_i Ln(X_i)\right] \quad (6)$$

Where s_0 and h_0 are entropy and enthalpy at the reference state.

The physical exergy quantifies the maximum useful work obtainable when the system state changes due to variation in pressure and temperature from the specific state (T,P) to reference state (T_0, P_0).

Table 1: Energy and exergy relations for the SCO_2/ORC system

Components	Energy relations	Exergy relations
Gas heater	$\dot{Q}_{GH} = \dot{m}_g(h_1 - h_2) = \dot{m}_{co2}(h_3 - h_{15})$	$\dot{E}_{D,GH} = (\dot{E}_1 + \dot{E}_{15}) - (\dot{E}_2 + \dot{E}_3)$
SCO_2 Turbine	$\dot{W}_{sco\,2,turb} = \dot{m}_{co2}(h_3 - h_4)$	$\dot{E}_{D,sco\,2\_turb} = \dot{E}_3 - (\dot{E}_4 + \dot{W}_{sco\,2,turb})$
Main Compressor	$\dot{W}_{MComp} = (1 - y) * \dot{m}_{co2}(h_{11} - h_{10})$	$\dot{E}_{D,Mcomp} = (\dot{E}_{10} + \dot{W}_{MComp}) - \dot{E}_{11}$
Recomp Compressor	$\dot{W}_{RComp} = y * \dot{m}_{co2}(h_{13} - h_7)$	$\dot{E}_{D,Rcomp} = (\dot{E}_7 + \dot{W}_{RComp}) - \dot{E}_{13}$
HTR	$(h_{15} - h_{14}) = (h_4 - h_5)$	$\dot{E}_{D,HTR} = (\dot{E}_4 + \dot{E}_{14}) - (\dot{E}_5 + \dot{E}_{15})$
LTR	$(1 - y) * (h_{12} - h_{11}) = (h_5 - h_6)$	$\dot{E}_{D,LTR} = (\dot{E}_5 + \dot{E}_{11}) - (\dot{E}_{12} + \dot{E}_6)$
Pre-cooler	$\dot{Q}_{PC} = \dot{m}_{co2}(h_9 - h_{10})$	$\dot{E}_{D,PC} = (\dot{E}_9 - \dot{E}_{10})$
Heat exchanger	$\dot{m}_{co2}(h_8 - h_9) = \dot{m}_{orc}(h_{19} - h_{18})$	$\dot{E}_{D,HX} = (\dot{E}_8 + \dot{E}_{18}) - (\dot{E}_9 + \dot{E}_{19})$
ORC Turbine	$\dot{W}_{ORC,turb} = \dot{m}_{orc}(h_{19} - h_{16})$	$\dot{E}_{D,ORC\_turb} = \dot{E}_{19} - (\dot{E}_{16} + \dot{W}_{ORC,turb})$
Pump	$\dot{W}_{Pump} = \dot{m}_{orc}(h_{18} - h_{17})$	$\dot{E}_{D,Pump} = (\dot{E}_{17} + \dot{W}_{Pump}) - \dot{E}_{18}$
Condenser	$\dot{Q}_{Cond} = \dot{m}_{orc}(h_{16} - h_{17}) = \dot{m}_{cool}(h_{17a} - h_{16a})$	$\dot{E}_{D,Cond} = (\dot{E}_{16} + \dot{E}_{16a}) - (\dot{E}_{17} + \dot{E}_{17a})$

The effectiveness of the HTR and LTR heat exchangers are expressed as[21]:

$$\varepsilon_{HTR} = (T_4 - T_5)/(T_4 - T_{14}) \quad (7)$$

$$\varepsilon_{LTR} = (T_5 - T_6)/(T_5 - T_{11}) \quad (8)$$

If minimum in hot side, or

$$\varepsilon_{LTR} = (T_{12} - T_{11})/(T_5 - T_{12}) \quad (9)$$

International Research Journal of Innovations in Engineering and Technology (IRJIET)

ISSN (online): 2581-3048

Volume 7, Issue 7, pp 165-177, July-2023

https://doi.org/10.47001/IRJIET/2023.707026

If minimum in cold side.

3.2 Performance evaluation parameters

The performance evaluation indexes for the combined SCO_2/ORC system are net power output ($\dot{W}_{net}$), thermal efficiency (η_{th}) and exergy efficiency (η_{ex}).

The net power output for the SCO_2 system is defined as:

$$\dot{W}_{net,sco\,2} = \dot{W}_{sco\,2,turb} - \dot{W}_{MComp} - \dot{W}_{RComp} \quad (10)$$

The net power output for the ORC system is:

$$\dot{W}_{net,ORC} = \dot{W}_{ORC,turb} - \dot{W}_{Pump} \quad (11)$$

Therefore, the combine net power output is expressed as:

$$\dot{W}_{net} = \dot{W}_{net,sco\,2} + \dot{W}_{net,ORC} \quad (12)$$

The thermal and exergy efficiency of the SCO_2/ORC system are expressed as:

$$\eta_{th} = \frac{\dot{W}_{net,sco\,2} + \dot{W}_{net,ORC}}{\dot{Q}_{IN}} \quad (13)$$

$$\eta_{ex} = \frac{\dot{W}_{net,sco\,2} + \dot{W}_{net,ORC}}{\dot{E}_{IN}} \quad (14)$$

Where $\dot{Q}_{IN}$ and $\dot{E}_{IN}$ defines the heat input and exergy input, respectively, for theSCO_2/ORC system from the exhaust waste gas. The heat input $\dot{Q}_{IN}$ is equal to the rate of heat transfer from the gas heater, $\dot{Q}_{GH}$.

The exergy input is defined as:

$$\dot{E}_{IN} = \dot{Q}_{IN}\left(1 - \frac{T_0}{T_3}\right) \quad (15)$$

The energy and exergy relations for each component of the SCO_2/ORC system is shown in Table 1.

3.3 Exergoeconomic model

The exergoeconomic approach, combines exergy and economic analyses to facilitate efficient and cost-effective design of energy systems. The method formulates cost-relations for evaluating cost of unit exergy at individual flow streams expressed as [19][22].

$$\sum \dot{C}_{i,k} + \dot{C}_{q,k} + \dot{Z}_k = \sum \dot{C}_{e,k} + \dot{C}_{w,k} \quad (16)$$

Where $\dot{C}_k = c_k E_k$

$\dot{C}_k, c_k, C_q$ and C_w represents cost rate of exergy $\left(\frac{\$}{hr}\right)$, cost of unit exergy of each stream $\left(\frac{\$}{GJ}\right)$, heat transfer rate of each component and work associated costs, respectively.

The overall system cost balance equation is expressed as

$$\dot{C}_{P,total} = \dot{C}_{F,total} + \dot{Z}_{total} \quad (17)$$

Where, $\dot{C}_P$, $\dot{C}_F$and $\dot{Z}$represents total product related costs, fuel cost rate and total costs related to capital investment and operation and maintenance.

The Investment cost rate ($\dot{Z}_k$) and annual levelized capital investment cost are expressed as follows:

International Research Journal of Innovations in Engineering and Technology (IRJIET)
ISSN (online): 2581-3048
Volume 7, Issue 7, pp 165-177, July-2023
https://doi.org/10.47001/IRJIET/2023.707026

$$\dot{Z}_k = \dot{Z}_k^{CI} + \dot{Z}_k^{OM} \quad (18)$$

$$\dot{Z}_k = \left(\frac{CRF}{\tau}\right) Z_k + \left(\frac{y_k}{\tau}\right) Z_k + \omega_k \dot{E}_{P,k} + \frac{R_k}{\tau} \quad (19)$$

Where $\left(\dot{Z}_J^{CI}\right)$ and $\left(\dot{Z}_J^{OM}\right)$ are capital investment and operation & maintenance costs, respectively. The capital investment for any k^{th} component is calculated with equations presented in **Appendix A**.

The capital recovery factor (CRF) is given as:

$$CRF = \frac{i_r(1+i_r)^n}{(1+i_r)^n - 1} \quad (20)$$

Where i_r and n denote the interest rate and the years of plant operation.

In **equation (19),** $\tau . y_k$ and ω_k represents the annual hours of plant operation, the fixed cost and the variable cost relating to operation and maintenance, respectively. Also in **equation (19),** the first term is significantly larger than the remaining terms, therefore the two last terms can be neglected.

Table 2 presents the cost balance and auxiliary cost relations for each component of the $RSCO_2$/ORC system.

Table 2: Component cost balance and auxiliary cost equations of the combined $RSCO_2$/ORC

Components	Cost balance
Gas heaters	$\dot{C}_{g1} + \dot{C}_{13} + \dot{Z}_{GH} = \dot{C}_{g2} + \dot{C}_1$ $c_1 = c_{13}$
SCO_2 Turb	$\dot{C}_1 + \dot{Z}_{SCO\ 2\_turb} = \dot{C}_2 + \dot{C}_{w,SCO\ 2\_turb}$ $c_2 = c_1;\ c_{w,sco\ 2\_turb} = c_{w,Recomp}$
HTR	$\dot{C}_2 + \dot{C}_{12} + \dot{Z}_{HTR} = \dot{C}_3 + \dot{C}_{13}$ $c_2 = c_3;\ c_{12} = c_{13}$
RComp	$\dot{C}_5 + \dot{C}_{w,Recomp} + \dot{Z}_{Recomp} = \dot{C}_{11}$ $c_{11} = c_5;$
Mixer	$\dot{C}_{11} + \dot{C}_{10} + \dot{Z}_{Mixer} = \dot{C}_{12}$
LTR	$\dot{C}_3 + \dot{C}_9 + \dot{Z}_{LTR} = \dot{C}_4 + \dot{C}_{10}$ $c_3 = c_4;\ c_9 = c_{10}$
MComp	$\dot{C}_8 + \dot{C}_{w,Mcomp} + \dot{Z}_{Mcomp} = \dot{C}_9$ $c_9 = c_8$
Separator	$\dot{C}_4 + \dot{Z}_{Sep} = \dot{C}_5 + \dot{C}_6$ $c_5 = c_4;\ c_6 = c_4$
Vapour Gen	$\dot{C}_6 + \dot{C}_{16} + \dot{Z}_{VG} = \dot{C}_7 + \dot{C}_{17}$ $c_6 = c_7$
ORC Turb	$\dot{C}_{17} + \dot{Z}_{ORC\_turb} = \dot{C}_{14} + \dot{C}_{w,ORC\_turb}$ $c_{17} = c_{14}$
ORC pump	$\dot{C}_{15} + \dot{C}_{w,ORC\_pump} + \dot{Z}_{ORC\_pump} = \dot{C}_{16}$ $c_{w,ORC\_turb} = c_{w,pump};c_{16} = c_{15}$

3.3.1 Exergoeconomic parameters

To evaluate the economic performance from both the whole system and individual component basis, two important exergoeconomic parameters; exergoeconomic factor (f_k) and cost of exergy destruction $\left(\dot{C}_{D,k}\right)$ are investigated.

- **Exergoeconomic factor**

Exergoeconomic factor (f_J)represents the proportion of capital investment and maintenance& operation costs in the exergy destruction related costs for each component [23]

$$f_k = \frac{\dot{Z}_k}{\dot{Z}_k + (\dot{C}_{D,k} + \dot{C}_{L,k})} \quad (21)$$

International Research Journal of Innovations in Engineering and Technology (IRJIET)

ISSN (online): 2581-3048

Volume 7, Issue 7, pp 165-177, July-2023

https://doi.org/10.47001/IRJIET/2023.707026

- **Cost of exergy destruction**

The cost of exergy destruction is often referred to as a hidden cost, as it does not appear in the cost balance equation of the components. The cost of exergy destruction, cost of product and cost of fuel can be expressed as follows [24].

$$\dot{C}_{D,k} = c_{f,k}\dot{E}_{D,k} \quad (22)$$

$$\dot{C}_{P,k} = c_{p,k}\dot{E}_{P,k} \quad (23)$$

$$\dot{C}_{F,k} = c_{f,k}\dot{E}_{F,k} \quad (24)$$

Where c_f and c_p denotes average cost per unit fuel and the cost per unit product for each component.

3.4 Model validation

The thermodynamic models of the SCO_2/ORC system being evaluated is first validated against available literature [13][14]. A comparison of the recompression SCO_2 thermodynamic properties and thermal efficiency in present work with those in literature [13][14] are presented in **Tables 3** and **4**, respectively. Results obtained from present model simulation are observed to have good agreement those reported in literature.

Table 3: Comparison of the results from present SCO_2 models with those reported by Ref. [13]

Point	P(MPa)			T(^{0}C)		
	Open source	Present work	Error (%)	Open source	Present work	Error (%)
1	25	25	0	379.65	380.0	+0.09
2	13.2	13.2	0	315.65	315.5	-0.05
3	13.2	13.2	0	189.25	183.0	-3.30
4	13.2	13.2	0	112.05	114.3	+1.96
5	13.2	13.2	0	112.05	114.3	+1.96
9	25	25	0	95.95	96.69	+0.76
10	25	25	0	163.65	169.1	+3.32
11	25	25	0	165.25	160.4	-3.02
12	25	25	0	165.25	168.8	+2.10
13	25	25	0	259.15	267.8	+3.33

Table 4: Comparison of thermal efficiencies for SCO_2/ORC system

Working fluids	Reference	Thermal efficiency		
		Reference study	Present study	Error (%)
CO_2/R123	Singh [13]	40.89%	41.16%	+0.66
CO_2/Isobutane	Besarati[14]	53.57%	54.20%	+1.17

4. Results and Discussion

This section evaluates the energy and exergy performance of the SCO_2/ORC system based on the input data in **Table 5.**A comparison between the performance of combined recompression-SCO_2/ORC system and the simple recompression-SCO_2 system is reported in **Table 6**and the simulation results obtain for SCO_2/ORC system is reported in **Table 7**. A sensitivity analysis is performed to investigate the effect of some key variables on the SCO_2/ORC system performance. In this work, the key parameters studied includes the turbine inlet temperature, compressor outlet pressure, SCO_2 mass flow rate, split mass flow rate, effectiveness of HTR and LTR, and organic working fluids.

4.1 Energy, exergy and exergoeconomic analysis

As previously mentioned, **Table 6** shows that the thermal (η_{th}) and exergy (η_{ex}) efficiencies of the combined SCO_2/ORC system are 52.52% and 70.42%, respectively, which are 3.19%pt. (percentage point) and 3.41 %pt. higher than the simple recompression-SCO_2 system. An additional 23 kW of power is produced compared to the SCO_2 system.

International Research Journal of Innovations in Engineering and Technology (IRJIET)

ISSN (online): 2581-3048

Volume 7, Issue 7, pp 165-177, July-2023

https://doi.org/10.47001/IRJIET/2023.707026

Table 5: SCO_2/ORC system Input data

Parameters	Value
Ambient temperature, T_{amb} (^{0}C)	25
Ambient pressure, P_{amb} (MPa)	0.101325
Compressor inlet temperature, T_8 (^{0}C)	65
Compressor outlet pressure, P_9 (MPa)	25
Compressor inlet pressure, P_8 (MPa)	13.2
Turbine inlet temperature, T_1 (^{0}C)	380
Compressor isentropic efficiency, η_{comp}	0.89
Turbine isentropic efficiency, η_{turb}	0.90
ORC turbine efficiency, $\eta_{ORC,turb}$	0.87
Pump isentropic efficiency, η_{pump}	0.85
HTR effectiveness, ε_{HTR}	0.95
LTR effectiveness, ε_{LTR}	0.95
Heat exchanger effectiveness, ε_{HX}	0.95
Pinch point temperature difference, ΔT_{HX} (^{0}C)	5
SCO_2 mass flow rate, $\dot{m}_{co2}$ (kg/s)	5
Split mass flow rate, $\dot{m}_{split}$ (kg/s)	2
ORC mass flow rate, $\dot{m}_{ORC}$ (kg/s)	2.3

Table 6: Comparison of performance parameters of the system

Parameters	SCO_2/ORC	SCO_2
$\dot{W}_{net}$ (kW)	378.70	355.7
$\dot{Q}_{in}$ (kW)	721.10	/
$\dot{E}_{in}$ (kW)	537.77	/
η_{th} (%)	52.52	49.33
η_{ex} (%)	70.42	67.01

SCO_2/ORC system because the low-grade waste heat released from the topping SCO_2 cycle is utilized to power the bottoming ORC cycle, therefore increasing the system's overall performance.

The thermodynamic properties, the mass flow rates and the exergy costs rates associated with fluid streams at each state point of the SCO_2/ORC system based on the input data listed in **Table 5** is presented in **Table 7**. **Fig.2** illustrates a summary of the actual exergy destruction and relative exergy destruction in each component of the system. It can be observed that the gas heater has the highest exergy destruction of 8.45kW which is 36.97% of the total exergy destroyed in the system. It is followed by the recompression compressor and SCO_2 turbine accounting for 3.93kW (17.17%) and 3.67kW (16.03%), respectively. This can be attributed to the low isentropic efficiencies associated with these components.

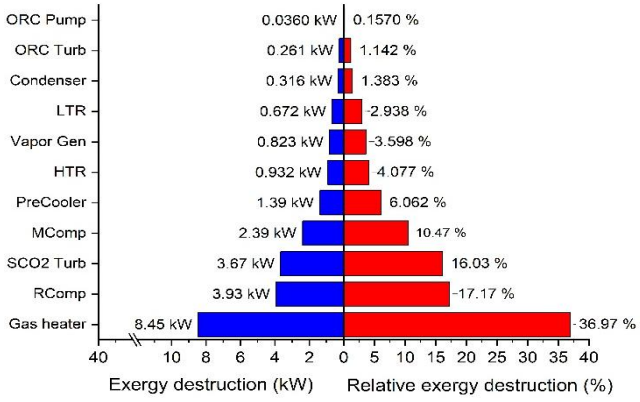

Fig.2: Absolute and relative exergy destruction in components of the system

International Research Journal of Innovations in Engineering and Technology (IRJIET)

ISSN (online): 2581-3048

Volume 7, Issue 7, pp 165-177, July-2023

https://doi.org/10.47001/IRJIET/2023.707026

Meanwhile, the ORC pump has the lowest exergy destruction of 0.036kW which account for only 0.157% of the total exergy destroyed in the system. It is followed by the ORC turbine and the condenser, accounting for 0.261kW (1.142%) and 0.316kW (1.383%), respectively. It can be observed that more exergy is destroyed in components of the topping cycle with higher temperatures and much lower exergy destruction experience in the components of the bottoming cycle with low operating temperatures.

Table 7: Thermodynamic property at all state point in the SCO_2/ORC system

State	Fluid	P (MPa)	T (^{0}C)	ṁ (kg/s)	h (kJ/kg)	s (kJ/kg-k)	Ė (kW)	Ċ ($/h)	c ($/GJ)
1	CO_2	25	380.0	5	819.5	2.404	3319	131.1	10.97
2	CO_2	10	289.6	5	736.3	2.437	2898	114.5	10.97
3	CO_2	10	189.0	5	619.4	2.208	2342	92.54	10.97
4	CO_2	10	123.1	5	537.1	2.016	1955	77.23	10.97
5	CO_2	10	123.1	2	537.1	2.016	782.0	30.89	10.97
6	CO_2	10	123.1	3	537.1	2.016	1173	46.34	10.97
7	CO_2	10	75.73	3	462.6	1.815	964.8	38.11	10.97
8	CO_2	10	57.00	3	415.3	1.675	833.1	41.00	13.67
9	CO_2	25	108.7	3	423.2	1.601	862.4	42.44	13.67
10	CO_2	25	185.0	3	560.4	1.930	1249	57.82	12.86
11	CO_2	25	181.8	2	555.5	1.920	823.6	32.54	10.97
12	CO_2	25	183.7	5	558.4	1.926	2073	90.36	12.11
13	CO_2	25	266.9	5	675.3	2.162	2628	112.5	11.89
14	R245fa	0.2038	34.00	1.8	355.7	1.515	399.8	16.61	11.54
15	R245fa	0.2038	34.00	1.8	244.5	1.153	215.9	8.972	11.54
16	R245fa	2.05	34.87	1.8	246.1	1.154	218.9	9.433	11.97
17	R245fa	2.05	118.7	1.8	370.1	1.508	426.2	17.71	11.54
7a	Water	0.1013	30.00	3.398	125.8	0.437	65.17	0.000	0.000
8a	Water	0.1013	40.00	3.398	167.6	0.572	195.8	2.770	3.930
14a	Water	0.1013	27.00	23.93	113.2	0.395	183.5	0.000	0.000
15a	Water	0.1013	29.00	23.93	121.6	0.423	367.1	7.711	5.835

Table 8: Results of exergy and exergoeconomic parameters of the SCO2/ORC system

Components	Exergy and exergoeconomic Parameters								
	$\dot{E}_p$ (kW)	$\dot{E}_f$ (kW)	$\dot{E}_D$ (kW)	c_p ($/GJ)	c_f ($/GJ)	$\dot{C}_{D,k}$ ($/h)	$\dot{Z}_k$ ($/h)	$\dot{Z}_k + \dot{C}_{D,k}$ ($/h)	f_k (%)
Gas heater	3319	3323	4.4510	10.97	10.95	0.1755	0.0820	0.2575	31.84
SCO_2 Turb	416.2	420.4	4.1180	11.40	10.97	0.1627	0.4797	0.6424	74.68
HTR	2628	2629	0.8243	11.89	11.87	0.0352	0.1844	0.2196	83.96
LTR	1249	1250	0.6383	12.86	12.83	0.0295	0.0719	0.1014	70.91
Recomp Comp	823.6	818.8	4.8070	10.97	10.80	0.1868	0.7116	0.8984	79.20
Main Comp	862.4	856.8	5.5500	13.67	13.41	0.2680	1.0670	1.3350	79.93
PreCooler	833.1	834.2	1.0370	13.67	13.61	0.0508	0.1162	0.1670	69.57
Vapour Gen	426.2	427.0	0.8888	11.54	11.48	0.0368	0.0502	0.0869	57.71
ORC Turb	26.00	26.32	0.3163	34.79	11.54	0.0131	2.1620	2.1760	99.40
Condenser	367.1	367.4	0.3193	5.835	5.777	0.0066	0.0697	0.0764	91.30
ORC pump	218.9	218.9	0.0362	11.97	11.86	0.0015	0.0887	0.0902	98.29

Table 8 present results of exergy and exergoeconomic analysis of the SCO_2/ORC system. The parameter $\dot{Z}_k + \dot{C}_{D,k}$ is used to evaluate the importance of each system component from the exergoeconomic view point, and implement potential improvement effort.Since in this study, the ORC turbine have the highest value of$\dot{Z}_k + \dot{C}_{D,k}$, it implies that the component is more important from exergoeconomic view point. Another important parameter is the exergoeconomic factor (f_k), which represents theratio of non-exergy related cost rate to the total cost rate [19]. It identifies the sources of major costs, whether from capital investment, operation and maintenance, or exergy destruction related costs. A high value of f_k indicates that, capital investment dominate the cost contribution in $\dot{Z}_k + \dot{C}_{D,k}$, and any further cost reduction can be obtain by using cheaper parts in the expense of component efficiency. On the other hand, a low value of f_k suggest that exergy destruction and operation and maintenance related costs dominates, any cost saving can be achieve by improving component efficiency even though it leads to increased capital investment.

International Research Journal of Innovations in Engineering and Technology (IRJIET)

ISSN (online): 2581-3048

Volume 7, Issue 7, pp 165-177, July-2023

https://doi.org/10.47001/IRJIET/2023.707026

Results from Table 8 reveals that the ORC turbine and main compressor have the highest value of $\dot{Z}_k + \dot{C}_{D,k}$, which indicate the component's level of importance in the SCO_2/ORC system. More so, the value of f_k for ORC turbine and main compressor are 99.40% and 79.93%, respectively, which are equally high indicating that the contribution of capital investment cost, $\dot{Z}_k$ in $\dot{Z}_k + \dot{C}_{D,k}$ dominants, therefore decreasing cost is obtainable by utilizing inexpensive parts at the expense of the component efficiency. The value of f_k in the bottoming ORC components except for the vapour generator are relatively high, suggesting that cost savings is possible through the use of components with lower capital investment cost. In the topping SCO_2, the f_k value of the components are high except for the gas heater with relatively low f_k value of 31.84% and $\dot{Z}_k + \dot{C}_{D,k}$ of 0.2575 ($/h), thus indicating that the contribution of cost associated with exergy destruction, $\dot{C}_{D,k}$ is higher for the gas heater, therefore component redesign and efficiency improvement effort is recommended.

4.1 Parametric Analysis

This analysis investigates the influence of major operating parameters on the thermodynamic and exergoeconomic performance of the SCO_2/ORC system. Fig.3 shows the effect of compressor outlet pressure (P_9) variation on the SCO_2/ORC system performance. Fig. 3(a) illustrates the influence of P_9 changes on electricity unit cost (c_{elect}), overall exergoeconomic factor ($f_{overall}$), overall exergy destruction cost rate ($\dot{C}_{D,overall}$), and $\dot{Z}_{overall} + \dot{C}_{D,overall}$ value. Fig. 3(b) shows the effect of P_9 on c_{elect}, net power output (W_{net}), thermal (η_{th}) and exergy (η_{ex}) efficiencies. In Fig. 3(a), it is observed that $\dot{C}_{D,overall}$ decrease first then increase as P_9 increases, the $\dot{Z}_{overall} + \dot{C}_{D,overall}$ values show steady increasing trend, c_{elect} decreases and $f_{overall}$, which represent the ratio of $\dot{Z}_{overall}$ and $\dot{Z}_{overall} + \dot{C}_{D,overall}$ increases at first and then decrease afterward, indicating there is an optimum value of P_9 at which $f_{overall}$ is maximum. This implies that increasing P_9 increases $\dot{Z}_{overall} + \dot{C}_{D,overall}$ and decrease $\dot{C}_{D,overall}$ with $\dot{Z}_{overall}$ dominating in the combination. Fig. 3(b) provide further explanation to this phenomenon. As P_9 increases, net power output (W_{net}), and thermal efficiency (η_{th}) increases, while electricity unit cost(c_{elect}), and exergy efficiency (η_{th}) decreases at constant $T_1 = 380^0$C. The net power output (W_{net}) of combinedSCO_2/ORC system increases with P_9, since the SCO_2 turbine work output is larger than the work associated with the main and recompression compressor.

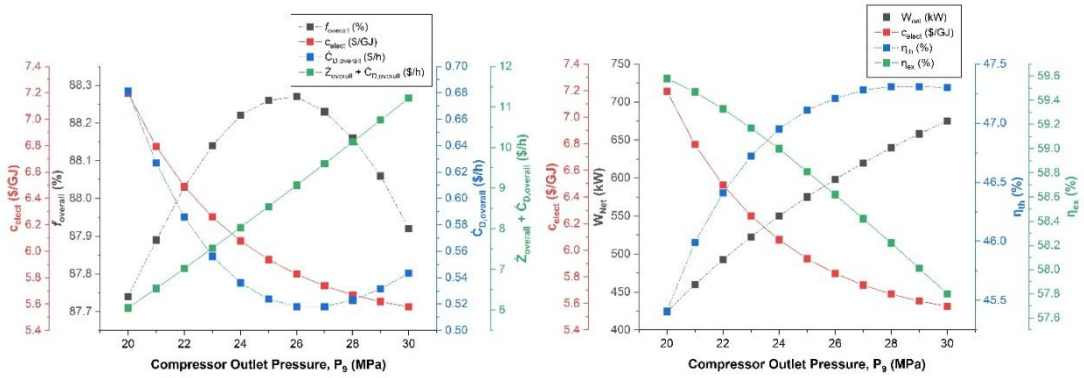

Fig.3: Effect of P_9 on (a)c_{elect}, $f_{overall}$, $\dot{C}_{D,overall}$ and$\dot{Z}_{overall} + \dot{C}_{D,overall}$, and (b)$c_{elect}$, W_{Net}, η_{th} andη_{ex}

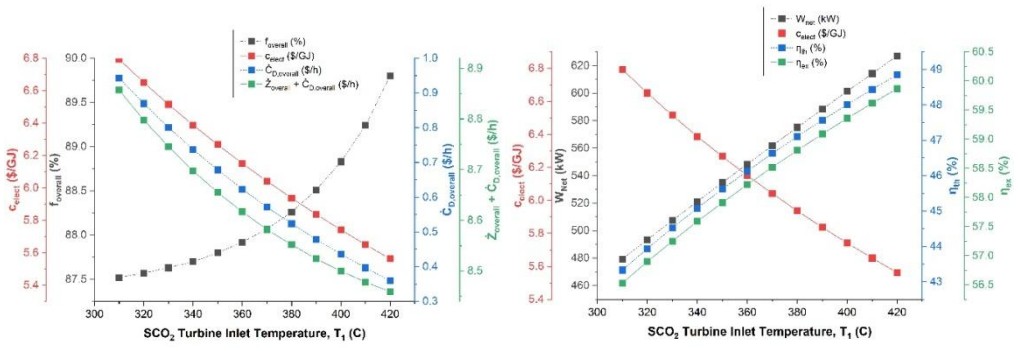

Fig.4: Effect of T_1 on (a)c_{elect}, $f_{overall}$, $\dot{C}_{D,overall}$ and$\dot{Z}_{overall} + \dot{C}_{D,overall}$, and (b)$c_{elect}$, W_{Net}, η_{th} andη_{ex}

International Research Journal of Innovations in Engineering and Technology (IRJIET)

ISSN (online): 2581-3048

Volume 7, Issue 7, pp 165-177, July-2023

https://doi.org/10.47001/IRJIET/2023.707026

Fig.4 illustrate the effect of SCO_2 turbine inlet temperature (T_1) on the performance and economics of the SCO_2/ORC system. In Fig.4(a), as T_1 increases, $f_{overall}$ increases gradually at first and then rapidly afterward, while c_{elect}, $\dot{C}_{D,overall}$, and $\dot{Z}_{overall} + \dot{C}_{D,overall}$ decreased gradually. The reason for this variation in exergoeconomic parameters with increase in T_1, is explained by the changes in performance parameters (W_{Net}, η_{th} and η_{ex}) in Fig. 4(b). As T_1 increases W_{Net}, η_{th} and η_{ex} increases gradually, indicating increase in energy and exergy input to the SCO_2/ORC system. The 1.355%pt. increase in T_1 from 310^0C to 420^0C, have resulted in a 0.06%pt., 0.035%pt and 1.4%pt. increase for η_{th}, η_{ex} and W_{Net}, respectively. The positive impact of this increase is attributed to the decrease of c_{elect}, $\dot{C}_{D,overall}$, and $\dot{Z}_{overall} + \dot{C}_{D,overall}$. The rise in $f_{overall}$ with increasingT_1, indicates that the $\dot{Z}_{overall}$ is dominant, which accounts for the use of more efficient components, leading to the subsequent lower electricity cost rate, c_{elect}.

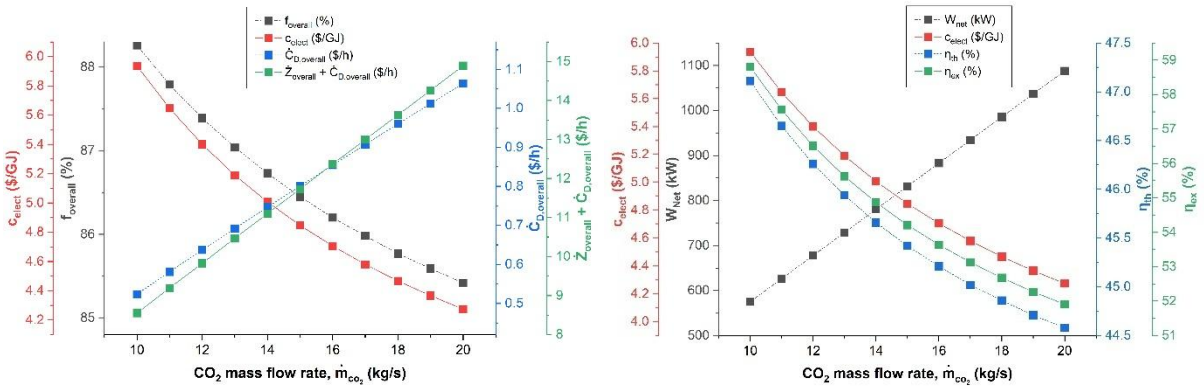

Fig.5: Effect of $\dot{m}_{co2}$ on (a)c_{elect}, $f_{overall}$, $\dot{C}_{D,overall}$ and$\dot{Z}_{overall} + \dot{C}_{D,overall}$, and (b)$c_{elect}$, W_{Net}, η_{th} andη_{ex}

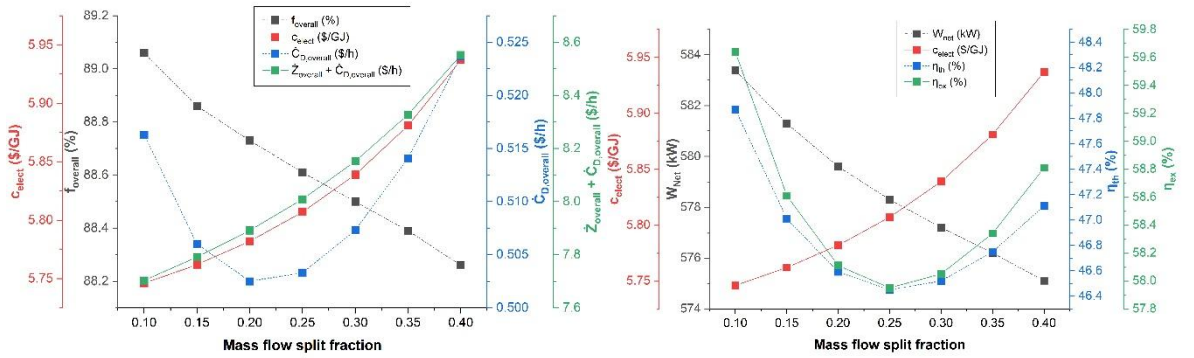

Fig.6: Effect of y_{split} on (a) c_{elect}, $f_{overall}$, $\dot{C}_{D,overall}$ and $\dot{Z}_{overall} + \dot{C}_{D,overall}$, and (b) c_{elect}, W_{Net}, η_{th} and η_{ex}

Fig.5 depicts the impact of CO_2 mass flow rate ($\dot{m}_{co2}$) variation on the system's performance and exergoeconomic parameters. Fig.5(a) illustrates a descending trend of $f_{overall}$ and c_{elect}, while $\dot{C}_{D,overall}$ and $\dot{Z}_{overall} + \dot{C}_{D,overall}$ show increasing trend as $\dot{m}_{co2}$ increases. In Fig.5(b), it can be observed that as $\dot{m}_{co2}$ increases, the value of W_{Net} increases, while η_{th}, η_{ex} and c_{elect} takes a descending trend. However, it is understandable that, as $\dot{m}_{co2}$ increases the W_{Net} also increases due to the increase cycle mass flow, and η_{th} and η_{ex} suffers because, given a constant input temperature, the energy and exergy content of the system decreases with rising $\dot{m}_{co2}$. The increasing $\dot{m}_{co2}$ leads to higher $\dot{C}_{D,overall}$ and $\dot{Z}_{overall}$ because of the declining η_{ex} and η_{th}, and higher investment cost due to larger components to accommodate the increase capacity. From exergoeconomic view point, decreasing $f_{overall}$ indicates further improvement through the use of more efficient components to decrease $\dot{C}_{D,overall}$ value, although it might increase investment cost.

International Research Journal of Innovations in Engineering and Technology (IRJIET)

ISSN (online): 2581-3048

Volume 7, Issue 7, pp 165-177, July-2023

https://doi.org/10.47001/IRJIET/2023.707026

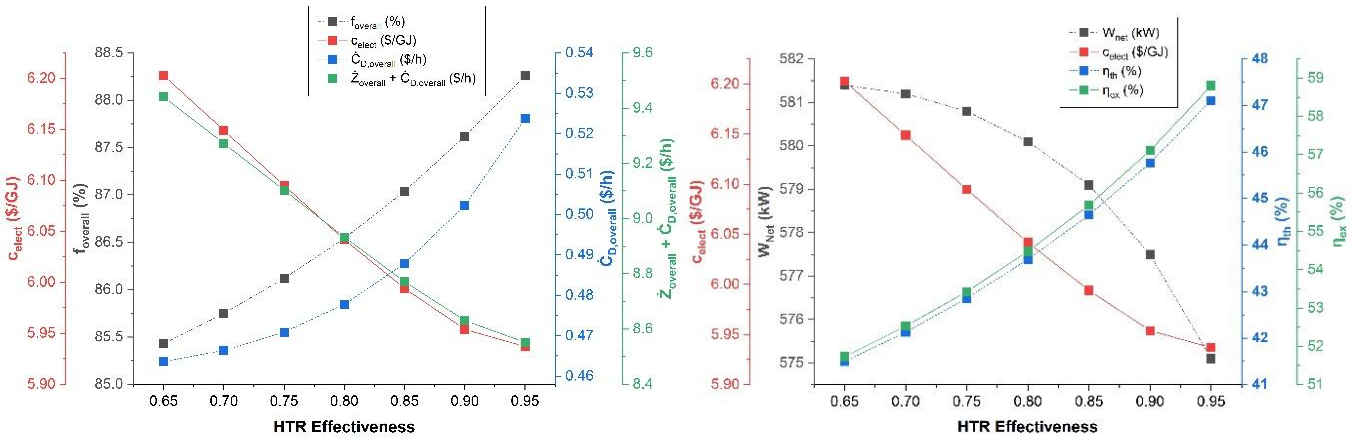

Fig.7: Effect of ε_{HTR} on (a)c_{elect}, $f_{overall}$, $\dot{C}_{D,overall}$ and$\dot{Z}_{overall} + \dot{C}_{D,overall}$, and (b)$c_{elect}$, W_{Net}, η_{th} and η_{ex}

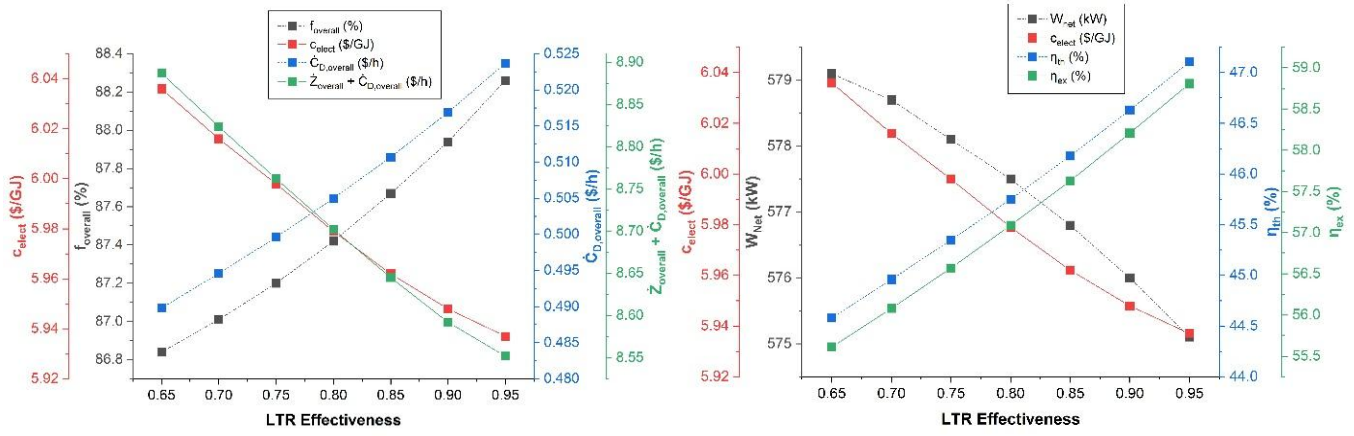

Fig.8: Effect of ε_{LTR} on (a)c_{elect}, $f_{overall}$, $\dot{C}_{D,overall}$ and$\dot{Z}_{overall} + \dot{C}_{D,overall}$, and (b)$c_{elect}$, W_{Net}, η_{th} and η_{ex}

Fig.6 shows the influence of mass flow split fraction (y_{split}) on the SCO_2/ORC system performance parameters. The y_{split} values range from 0.1 to 0.4. As y_{split} increases, $f_{overall}$ decreases, c_{elect} and $\dot{Z}_{overall} + \dot{C}_{D,overall}$ increases, while $\dot{C}_{D,overall}$ is observed to decrease at first and then increase afterward, as shown in Fig.6(a). In Fig.6(b), as y_{split} increases, W_{Net} decreases, c_{elect} increases and the values of η_{th} and η_{ex} decreased at first and then increased afterward.

The effect of HTR effectiveness (ε_{HTR}) on the system's performance and exergoeconomic parameter is illustrated in Fig.7. The values of c_{elect} and $\dot{Z}_{overall} + \dot{C}_{D,overall}$ are observed to decrease, while , $f_{overall}$ and $\dot{C}_{D,overall}$ display a rising trend as ε_{HTR} increases, as shown in Fig.7(a). On the other hand, Fig.7(b) shows ε_{HTR}, W_{Net} and η_{th}, η_{ex} decreasing and increasing trends, respectively.This indicates that as ε_{HTR} increases, there is increased heat transfer, exergy gains and decrease in exergy destruction in the system. Another reason for the increase in exergy efficiency is that the net exergy output from the system is relatively constant because parameters such as cycle pressure ratio, isentropic efficiency and other operating conditions are unaffected by increasing ε_{HTR}, hence, the increase inη_{ex}. From exergoeconomic view point, decreasing $f_{overall}$ indicates increasing $\dot{C}_{D,overall}$ due to higher heat transfer and exergy content in the system as ε_{HTR} increases. Fig.8(a-b) depicts the influence of ε_{LTR} variation on the system's performance and exergoeconomic parameters. The trend experienced strongly follow previous explanation in Fig.7.

ISSN (online): 2581-3048
Volume 7, Issue 7, pp 165-177, July-2023
https://doi.org/10.47001/IRJIET/2023.707026

5. Conclusion

The paper evaluates the energy, energy and exergoeconomic performance analyses of a recompression SCO_2/ORC system for exhaust waste heat recovery application. Analysis indicates that SCO_2/ORC system has higher thermal and exergy efficiency by 3.19%pt. and 3.41%pt. compared to the single SCO_2 system. Results reveal that for a 10kPa increase in input pressure (P_1), W_{Net}, η_{th} and $\dot{Z}_{overall} + \dot{C}_{D,overall}$ increases by 251.3kW, 1.89%pt. and 5.165h/GJ respectively, and decreases η_{ex} and c_{elect} by 1.89%pt. and 1.618$/GJ. Another interesting parameter is T_1, which shows that increasing the value of T_1 terns to increase W_{Net}, η_{th}, η_{ex} and $f_{overall}$, while a decreasing trend is observed for c_{elect}, $\dot{C}_{D,overall}$ and $\dot{Z}_{overall} + \dot{C}_{D,overall}$. The SCO_2 mass flow rate ($\dot{m}_{co2}$) affects system sizing, performance and economics. It was observed that only10kg/s increase in $\dot{m}_{co2}$ at constant T_1 and P_1 condition could increase the value of W_{Net} by 512.9kW, and decrease η_{th}, η_{ex} and c_{elect} by 2.53%pt., 6.9%pt. and 1.663$/GJ, respectively. It can also be observed that ε_{LTR} and ε_{HTR} have significant influence on the system performance and exergoeconomic, with similar trends. Increasing the value, indicate a simultaneous increase in η_{th}, η_{ex} and decrease in W_{Net}, c_{elect}, respectively. Finally, the study analyses the impact of different parameters on system energy, exergy and exergoeconomic performance. However, to obtain a cost-effective system, optimization of the system to determine optimum decision parameters is required, thus further research is recommended in that direction.

REFERENCES

[1] Kim, Y. M., Sohn, J. L. and Yoon, E. S. (2017) 'Supercritical CO2 Rankine cycles for waste heat recovery from gas turbine', *Energy*. Elsevier Ltd, 118, pp. 893–905. doi: 10.1016/j.energy.2016.10.106.

[2] Song, J., Li, X. song, Ren, X. dong and Gu, C. wei (2018) 'Performance improvement of a preheating supercritical CO2 (S-CO2) cycle based system for engine waste heat recovery', *Energy Conversion and Management*. Elsevier, 161(February), pp. 225–233. doi: 10.1016/j.enconman.2018.02.009.

[3] Sarkar, J. (2009) 'Second law analysis of supercritical CO2 recompression Brayton cycle', *Energy*. Elsevier Ltd, 34(9), pp. 1172–1178. doi: 10.1016/j.energy.2009.04.030.

[4] Ahn, Y., Bae, S. J., Kim, M., Cho, S. K., Baik, S., Lee, J. I. and Cha, J. E. (2015) 'ScienceDirect REVIEW OF SUPERCRITICAL CO 2 POWER CYCLE TECHNOLOGY', *Nuclear Engineering and Technology*. Elsevier B.V, (August), pp. 1–15. doi: 10.1016/j.net.2015.06.009.

[5] Guo, Z., Zhao, Y., Zhu, Y., Niu, F. and Lu, D. (2018) 'Progress in Nuclear Energy Optimal design of supercritical CO 2 power cycle for next generation nuclear power conversion systems', *Progress in Nuclear Energy*. Elsevier, 108(October 2017), pp. 111–121. doi: 10.1016/j.pnucene.2018.04.023.

[6] Moullec, Y. Le (2013) 'Conceptual study of a high efficiency coal-fired power plant with CO2 capture using a supercritical CO_2 Brayton cycle', *Energy*. Elsevier Ltd, 49, pp. 32–46. doi: 10.1016/j.energy.2012.10.022.

[7] Mecheri, M. and Le, Y. (2016) 'Supercritical CO 2 Brayton cycles for coal- fi red power plants', *Energy*. Elsevier Ltd, 103, pp. 758–771. doi: 10.1016/j.energy.2016.02.111.

[8] Ruiz-casanova, E., Rubio-maya, C., Pacheco-ibarra, J. J., Ambriz-díaz, V. M., Romero, C. E., Wang, X., Engineering, M., Michoacana, U., Nicolás, D. S. and Michoacán, C. P. (2020) 'Thermodynamic analysis and optimization of supercritical carbon dioxide Brayton cycles for use with low-grade geothermal heat sources', *Energy Conversion and Management*. Elsevier, 216(May), p. 112978. doi: 10.1016/j.enconman.2020.112978.

[9] Song, J., Wang, Y., Wang, K., Wang, J. and Markides, C. N. (2021) 'Combined supercritical CO 2 (SCO 2) cycle and organic Rankine cycle (ORC) system for hybrid solar and geothermal power generation : Thermoeconomic assessment of various con fi gurations', *Renewable Energy*. Elsevier Ltd, 174, pp. 1020–1035. doi: 10.1016/j.renene.2021.04.124.

[10] Wang, K. and He, Y. (2017) 'Thermodynamic analysis and optimization of a molten salt solar power tower integrated with a recompression supercritical CO 2 Brayton cycle based on integrated modeling', *Energy Conversion and Management*. Elsevier Ltd, 135, pp. 336–350. doi: 10.1016/j.enconman.2016.12.085.

[11] Milani, D., Tri, M., Mcnaughton, R. and Abbas, A. (2017) 'Optimizing an advanced hybrid of solar-assisted supercritical CO_2 Brayton cycle : A vital transition for low-carbon power generation industry', *Energy Conversion and Management*. Elsevier Ltd, 148, pp. 1317–1331. doi: 10.1016/j.enconman.2017.06.017.

[12] Acikkalp, E. (2017) 'Ecologic and sustainable objective thermodynamic evaluation of molten carbonate fuel cell e supercritical CO 2 Brayton cycle hybrid system', *International Journal of Heat and Mass Transfer*, pp. 1–9. doi: 10.1016/j.ijhydene.2016.12.110.

[13] Singh, H. and Mishra, R. S. (2018) 'Energy- and exergy-based performance evaluation of solar powered

ISSN (online): 2581-3048
Volume 7, Issue 7, pp 165-177, July-2023
https://doi.org/10.47001/IRJIET/2023.707026

combined cycle (recompression supercritical carbon dioxide cycle / organic Rankine cycle)', *Clean Energy*, 2(2), pp. 140–153. doi: 10.1093/ce/zky011.

[14] Besarati, S. M. and Goswami, D. Y. (2014) 'Analysis of Advanced Supercritical Carbon Dioxide Power Cycles With a Bottoming Cycle for Concentrating Solar Power Applications', 136(February), pp. 2–8. doi: 10.1115/1.4025700.

[15] Akbari, A. D. and Mahmoudi, S. M. S. (2014) 'Thermoeconomic analysis & optimization of the combined supercritical CO_2 (carbon dioxide) recompression Brayton/organic Rankine cycle', *Energy*. Elsevier Ltd, 78, pp. 501–512. doi: 10.1016/j.energy.2014.10.037.

[16] Wang, X. and Dai, Y. (2016) 'Exergoeconomic analysis of utilizing the transcritical CO2 cycle and the ORC for a recompression supercritical CO2 cycle waste heat recovery: A comparative study', *Applied Energy*. Elsevier Ltd, 170, pp. 193–207. doi: 10.1016/j.apenergy.2016.02.112.

[17] Cao, Y., Habibi, H., Zoghi, M. and Raise, A. (2021) 'Waste heat recovery of a combined regenerative gas turbine - recompression supercritical CO 2 Brayton cycle driven by a hybrid solar-biomass heat source for multi-generation purpose : 4E analysis and parametric study', *Energy*. Elsevier Ltd, 236, p. 121432. doi: 10.1016/j.energy.2021.121432.

[18] S. A. Klein (2020) 'Engineering Equation Solver'. F-Chart Software.

[19] Bejan, A., Tsatsaronis, G. and Moran, M. (1996) *Thermal Design & Optimization*. New York: John Wiley & sons Inc.

[20] Igbong, D., Nyong, O. E., Enyia, J. and Agba, A. (2021) 'Working Fluid Selection for Simple and Recuperative Organic Rankine Cycle Operating Under Varying Conditions : A Comparative Analysis', *Advances in Science and Technology Research Journal*, 15(4), pp. 202–221.

[21] Igbong, D. (2022) 'Energy and Exergy-based Performance Analysis of a Combined Recompression Supercritical Carbon Dioxide-Organic Rankine Cycle for Waste Heat Recovery', *Cleaner Energy Systems*, p. 100022.

[22] Igbong, D., Nyong, O., Enyia, J., Oluwadare, B. and Obhua, M. (2021) 'Exergoeconomic Evaluation and Optimization of Dual Pressure Organic Rankine Cycle (ORC) for Geothermal Heat Source Utilization', *Journal of power and energy engineering*, 9(9), pp. 19–40. doi: 10.4236/jpee.2021.99002.

[23] Shokati, N., Ranjbar, F. and Yari, M. (2015) 'Exergoeconomic analysis and optimization of basic , dual-pressure and dual- fl uid ORCs and Kalina geothermal power plants : A comparative study', *Renewable Energy*. Elsevier Ltd, 83, pp. 527–542. doi: 10.1016/j.renene.2015.04.069.

[24] Ahmadzadeh, A., Reza, M. and Sedaghat, A. (2017) 'Thermal and exergoeconomic analysis of a novel solar driven combined power and ejector refrigeration (CPER) system', *International Journal of Refrigeration*. Elsevier Ltd. doi: 10.1016/j.ijrefrig.2017.07.015.

Citation of this Article:

Oku Ekpenyong Nyong, "Energy, Exergy, and Exergoeconomic Analysis of a Combined Recompression Supercritical Carbon Dioxide Brayton-Organic Rankine Cycle for Waste Heat Recovery" Published in *International Research Journal of Innovations in Engineering and Technology - IRJIET*, Volume 7, Issue 7, pp 165-177, July 2023. Article DOI https://doi.org/10.47001/IRJIET/2023.707026

****

